

Magnetoresistance of Thin-Film NiFe Devices Exhibiting Single-Domain Behavior

R. W. Cross, J. O. Oti, S. E. Russek, and T. Silva

Electromagnetic Technology Division, National Institute of Standards and Technology, Boulder, Colorado 80303

Y. K. Kim

Quantum Peripherals Colorado, Inc.*, Louisville, Colorado 80028-8188

Abstract— Rectangular NiFe stripes as small as $1 \times 5 \mu\text{m}$ were fabricated and characterized as a function of film thickness. Gold current leads were sputtered and patterned onto the stripes so that magnetoresistance measurements could be performed. A uniform in-plane magnetic field was applied transverse to the stripe length and at various angles from the perpendicular direction. For film thicknesses greater than 10 nm, the magnetoresistance for all of the devices had large jumps and hysteresis due to domain formation. As the thickness of the film decreased below 10 nm, the domain structure disappeared for stripe heights $2 \mu\text{m}$ or less. Theoretical calculations of the magnetization reversals were obtained using a numerical implementation of the Stoner-Wohlfarth model for the switching of a single-domain ellipsoidal particle. The calculations were used to predict the switching field where the magnetization reaches an unstable threshold, causing a jump in the magnetization and magnetoresistance. The model was in close agreement with experimental results for various field orientations.

I. INTRODUCTION

The formation of domains in anisotropic magnetoresistive (AMR) materials has long been a source of noise in thin-film magnetic field sensors. The presence of longitudinal fields, due to magnetic poles or a component of the external magnetic field, can destabilize the single-domain state, breaking it into multiple domains [1]–[3]. In magnetic read-head applications, the field from the bits can cut through the device at angles up to 15° from the transverse direction. For long, rectangular, thin-film stripes with a field-induced easy axis along the stripe length, the magnetization remains single-domain for fields applied transversely to the stripe length. However, when the field is applied with a slight longitudinal component, a three-domain state may form due to an easy-axis reversal of the central magnetization region [1], [2]. A Kerr image of the three-domain structure is shown in Fig. 1(a) at $H = -4 \text{ kA/m}$ (-50 Oe) for an $8 \times 8 \mu\text{m}$ device (active area), 25 nm thick, and with a misalignment angle of 1.4° (measured from transverse). The edge domains are directed toward the right (initial direction) and the central domain is aligned to the left. Plots of the AMR response for the device are shown in Fig. 1(b) for different field angles. The response becomes more hysteretic for angles greater than 1.4° due to a more complicated domain structure.

In this work, we study the effect of film thickness on the formation of domains in NiFe thin-film devices with stripe heights less than $2 \mu\text{m}$. For film thickness less than 10 nm, Barkhausen jumps in the MR response disappear, due to the elimination of domains. This occurs because of the increase in transition width for the in-plane rotation of a Néel domain wall, which is determined by the competition between exchange, anisotropy, and magneto-

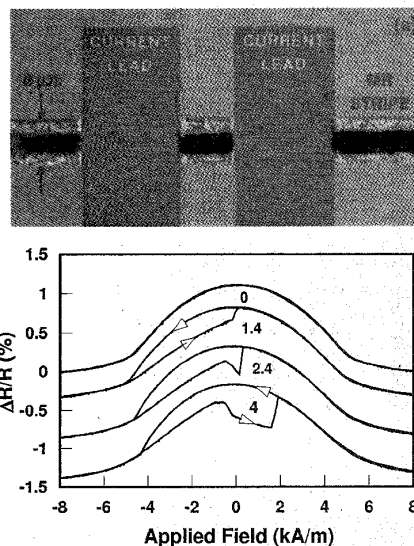


Fig. 1. (a) A Kerr image of the three-domain state in a $8 \times 8 \mu\text{m}$ (active area) device with a film thickness of 25 nm and a field angle of 1.4° . (b) MR response at different field angles from 0 to 4° . The curves have been shifted.

static energies. The expression for the energy density of an ellipsoidal-cylinder Néel wall is given by [4]

$$E_N = \frac{A\pi^2}{\delta} + \frac{K\delta}{2} + \frac{t\delta M_s^2}{4(\delta + t)} \quad (1)$$

where A is the exchange constant, δ is the domain-wall transition width, K is the anisotropy constant, t is the thickness, and M_s is the saturation magnetization. To determine the wall transition width, the energy expression (1) must be minimized with respect to δ . The effect of exchange is to reduce the rate of magnetization rotation by spreading out the width of the wall transition, whereas magnetocrystalline or induced anisotropy tends to restrict the width of the transition. In addition, the magnetostatic energy of a wall depends on the film thickness, leading to a thickness dependence of δ . The wall width increases as the film thickness decreases and has been calculated to be about $1 \mu\text{m}$ for thicknesses of 10 nm for NiFe [5], [6]. We measured and modeled the magnetization and MR response for devices small enough to be in this single-domain state when the wall width is on the order of the stripe height. We found that a simple numerical implementation of the Stoner-Wohlfarth model [7] accurately describes the measured magnetic behavior, which in turn can be used to calculate the AMR response. This simple calculation can be performed without having to use a complicated micromagnetic model.

Manuscript received February 17, 1995. Contribution of the National Institute of Standards and Technology, not subject to copyright.

II. RESULTS

Sputtered $\text{Ni}_{81}\text{Fe}_{19}$ thin films on Si wafers were fabricated into two-terminal rectangular test devices with thicknesses ranging from 5 to 25 nm. The stripe height of the devices varied from 1 to 16 μm and the stripe length varied from 5 to 120 μm . The active area of a device is defined as the stripe height times the track width (the separation between the current leads, which ranged from 1 to 32 μm). The external field was applied in the plane of the film at different angles, measured relative to the transverse direction. The resistance was measured with a calibrated current source and a nanovoltmeter. For thicknesses greater than 10 nm or stripe heights greater than 2 μm , the response was similar to that shown in Fig. 1(b). The response was reversible for transverse fields ($\phi = 0^\circ$), and hysteresis formed due to domain formation for $\phi > 0^\circ$. For large misalignment angles ($\phi > 5^\circ$), the output had multiple peaks and hysteresis due to the formation of a large number of domains.

When the thickness of the film was 10 nm or less and the stripe height was 2 μm or smaller, the response of the device changed to single-domain behavior. As the field was swept from negative to positive values, the Barkhausen jump, such as that seen in Fig. 1(b) for $\phi > 0^\circ$, was not present for field angles up to 15° . The measured MR for a NiFe device with a track width of 1 μm (overall length of 5 μm), a stripe height of 1 μm , a film thickness of 5 nm, and a field angle of 15° is shown in Fig. 2 (a). The jumps in the response are due to the switching of the magnetization rather than domain-wall motion and annihilation. The corresponding transverse component of magnetization M_y can be calculated from the angle θ between the magnetization and the current, given by the relation for the change in resistivity ρ ,

$$\rho = \rho_0 - \Delta\rho \cos^2\theta, \quad (2)$$

where $\Delta\rho$ is the characteristic MR of the material and ρ_0 is the resistivity at zero field.

The magnetic behavior of the device is sketched in Fig. 3. At point 1 in the R-H curve, the magnetization is saturated along the field direction, which is at a maximum negative value. As the field is swept toward positive values, the magnetization aligns along a minimum energy position, which involves the shape, external field, and anisotropy energies. At point 2, the magnetization reaches an unstable energy configuration and switches (or snaps) from M to M' , resulting in a jump in the MR response at $2'$. The longitudinal component of applied field drives the magnetization over to the new, stable energy state. The magnetization is again saturated at point 3 along the field direction. The entire process is then repeated for the field sweep from positive to negative fields, with the jump now occurring for negative field values (the magnetization rotates around in a circular motion with field cycle).

The MR response was measured for the same $1 \times 1 \mu\text{m}$ device as a function of applied field angle from 0 to 15° , shown in Fig. 4. With increasing field angle, the switching field decreases due to the increase of the longitudinal field component, which causes a faster rotation of the magnetization. This dependence on field angle is very different from what was observed for the thicker devices ($> 10 \text{ nm}$), which behaved much like what is shown in Fig. 1(b). For example, there are two symmetric jumps for the single-domain case because of the circular rotation of the magnetization with field cycle, whereas the multiple-domain case exhibits only a single jump. In addition, the jumps move towards lower field with increasing angle for the single-domain devices, whereas the jump grows and the response deteriorates for the multiple-domain devices.

III. THEORY

We have extended a previously described Stoner-Wohlfarth model of a uniformly magnetized ellipsoid [7] by including a uniaxial magnetocrystalline anisotropy energy term in addition to the demagnetizing and external applied field terms in the expression for the total energy. The total energy density is given by

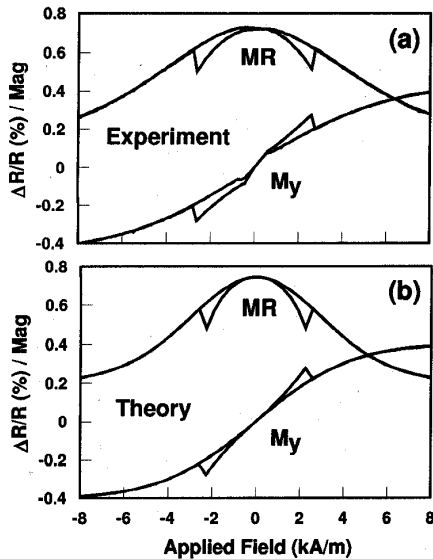


Fig. 2. Plots of MR versus field with the corresponding magnetization loop for a misalignment angle of 15° for (a) experimental results, and (b) theoretical calculations for a $1 \times 1 \mu\text{m}$ (active area) device with a film thickness of 5 nm. The magnetization curves are in arbitrary units and are plotted with the MR curves.

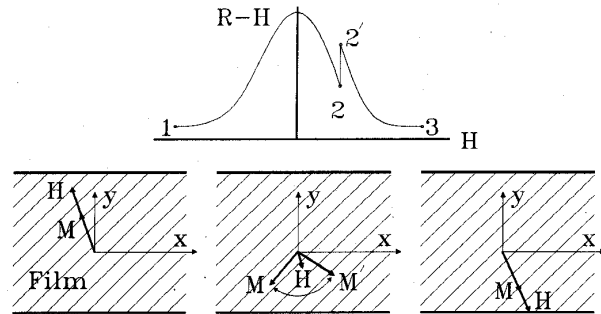


Fig. 3. Schematic diagram of the magnetic behavior of an MR device. A jump in MR occurs from point 2 to $2'$ due to the jump in magnetization from M to M' .

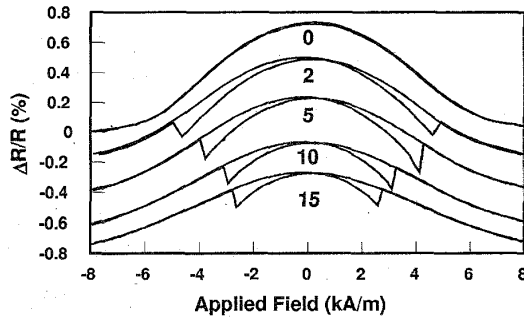


Fig. 4. Experimental MR curves for the $1 \times 1 \mu\text{m}$ (active area) device with a thickness of 5 nm as a function field angle from 0 to 15° .

$$W = \frac{1}{2}M_s^2(N_x\alpha^2 + N_y\beta^2 + N_z\gamma^2) - H_0M_s(l\alpha + m\beta + n\gamma) + \frac{1}{2}H_kM_s(1-\gamma^2), \quad (3)$$

where α , β , and γ are direction cosines of the magnetization M_s ; l , m , and n are direction cosines of the applied field H_0 ; N_x , N_y , and N_z ($N_x + N_y + N_z = 1$) are the demagnetizing factors along the three principal axes; $H_k = 2K/M_s$ is the magnetic anisotropy field and K is the magnetic anisotropy constant. The terms α , β , and γ are related to the azimuthal and polar angular coordinates of the magnetization vector θ_M , ϕ_M by $\alpha = \sin\theta_M \cos\phi_M$, $\beta = \sin\theta_M \sin\phi_M$, and $\gamma = \cos\theta_M$.

For a fixed external field direction, the expressions in parentheses in (3) can be computed as functions of θ_M and ϕ_M and then stored. For varying field directions, the term $(l\alpha + m\beta + n\gamma)$ needs to be continually updated. The stored values are used to compute the energy functional $W(\theta_M, \phi_M)$ according to (3), and the angular coordinates that yield the minimum energy value corresponds to the sought-after orientation of the magnetization vector for a given applied field. It is possible to tabulate the values used in the computation only for one quadrant of space; the solution in other quadrants can then be found by symmetry. In addition, the solution space depends on the history of the magnetization process, and solutions corresponding to $\theta_M = 0$ must be treated specially. These issues are described in detail in [7]. The following parameters were used in the calculations presented in this article: saturation

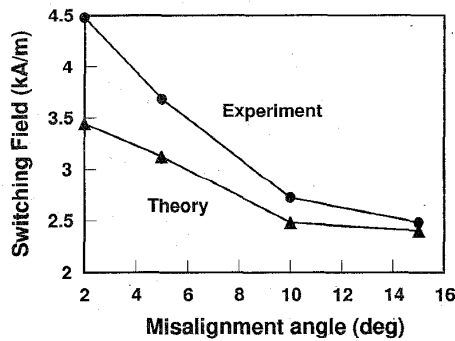


Fig. 5. Plot of the field where the magnetization switches as a function of field angle for both theory and experiment for the $1 \times 1 \mu\text{m}$ (active area) device.

magnetization $M_s = 500 \text{ kA/m}$; in-plane and out-of-plane demagnetizing factors $N_y = N_z = 0$ and $N_x = 1$; anisotropy field along the long axis (z -axis) of the film $H_k = 4 \text{ kA/m}$. The corresponding theoretical calculations for the experimental results of Fig. 2(a) are shown in Fig. 2(b).

The switching of the magnetization occurs as the free energy reaches an unstable threshold, changing from a minimum to a maximum energy state. Both the theoretical and experimental values of the switching field are shown in Fig. 5 for the $1 \times 1 \mu\text{m}$ (active area) device. The theoretical calculations are in close agreement with the measured values. Discrepancies may arise due to the expected nonuniform rotation of the magnetization at the edges compared to the central region of the film.

IV. SUMMARY

We measured the MR response of NiFe devices as a function of film thickness and found that domain formation disappeared for thicknesses less than 10 nm and for stripe heights 2 μm or less. A numerical implementation of a Stoner-Wohlfarth model was used to determine the magnetic behavior of the single-domain rotation of a $1 \times 1 \mu\text{m}$ device, and good agreement was found with experiment. For a stripe height of 1 μm , the optimum thickness was found to be approximately 10 nm. This gives the largest $\Delta R/R$ ratio of approximately 1.2% with single-domain behavior. ($\Delta R/R$ begins to decrease rapidly for thicknesses less than 10 nm because of the increase in resistivity due to surface scattering. This occurs because the thickness is on the order of the mean-free-path of the electron.) Magnetic recording read-head technology may employ this effect to eliminate domain-stabilization schemes. If one of these elements is biased to the midpoint of the response and the net field never crosses zero, the output should be reversible. The results may apply to spin-valve devices where each thin magnetic layer may be treated as single domain, interacting through magnetostatic and exchange fields. To treat the spin-valve case, the minimum energy configuration of each layer can be calculated, including the interaction of the other layer, and then iterated until a stable solution can be found.

REFERENCES

- [1] R. W. Cross, A. B. Kos, C. A. Thompson, T. W. Petersen, and J. A. Brug, "Local magnetoresistive response in thin-film read elements: A sub-micrometer-resolution measurement system," *IEEE Trans. Magn.*, vol. 28, pp. 3060-3065, September 1992.
- [2] N. Smith, "A specific model for domain-wall nucleation in thin-film Permalloy microelements," *J. Appl. Phys.*, vol. 63, pp. 2932-2937, April 1988.
- [3] C. Tsang and S. K. Decker, "Study of domain formation in small Permalloy magnetoresistive elements," *J. Appl. Phys.*, vol. 53, pp. 2602-2604, March 1982.
- [4] D. J. Craik and R. S. Tebble, *Ferromagnetism and Ferromagnetic Domains*, in Selected Topics in Solid State Physics, vol. IV, E. P. Wohlfarth, Ed., John Wiley and Sons, Inc., New York, pp. 24-31, 1965.
- [5] R. F. Soohoo, *Magnetic Thin Films*, Harper and Row, New York, pp. 40-45, 1965.
- [6] S. Middelhoek, "Domain walls in thin NiFe films," *J. Appl. Phys.*, vol. 34, pp. 1054-1059, 1963.
- [7] C. E. Johnson, "Single-domain magnetization curves for general ellipsoid," *J. Appl. Phys.*, vol. 33, pp. 2515-2518, 1962.

* Formally known as Rocky Mountain Magnetics, Inc.